

Electronic structures of silicon nitride revealed by tight binding calculations

A.N. Sorokin^a, A.A. Karpushin^a, V.A. Gritsenko^a, Hei Wong^{b,*}

^a Institute of Semiconductor Physics, Novosibirsk 630090, Russia

^b Department of Electronic Engineering, City University of Hong Kong, Tat Chee Avenue, Kowloon, Hong Kong

Received 9 October 2006; received in revised form 18 April 2007

Available online 21 September 2007

Abstract

A new tight binding (TB) potential model was proposed for determining the electronic structures of ionic–covalent materials. In the TB model, the matrix elements were determined from the atomic characteristics of the crystal. The atomic parameters of the solid were determined based on the general quantum principles and no adjustable parameter was needed. Electronic structures of amorphous silicon nitride (Si_3N_4) were calculated using this method. A good agreement between the calculated and experimental values in terms of fundamental properties such as the position of the valence-band edge, the conduction-band edge, and the energy bandgap were obtained. Charge transfer between the silicon and nitrogen atoms was also precisely calculated in this work.

© 2007 Elsevier B.V. All rights reserved.

PACS: 71.15.–m; 71.15.Mb; 77.55.+f

Keywords: Dielectric properties, relaxation, electric modulus; Modeling and simulation

1. Introduction

Non-empirical *ab initio* calculation has now become a major tool for studying the electronic structures of solids. As no empirical parameter is needed, the calculation results are found to be more reliable. However, there are several computational difficulties involved with the non-empirical methods. The major difficulty is that the charge transfer between atoms for forming the chemical bonds in the solid must be taken into account for ionic and ionic–covalent crystals or for crystals containing charged impurities. As the charge transfers in crystals and the nature of amorphous materials normally involve rather large volumes, a larger number of basis functions and hence a larger memory required in the *ab initio* calculations. In some calculations, e.g., *ab initio* calculations based on some clusters, artificial localization of charges within the clusters were

used and are often found to be inadequate for dealing the effects of charge transfer. In some other cases, periodic models were used but these models were also found to be inappropriate for calculating the defect structures in solids. Because of the requirement of electrical neutrality in the cells, artificial compensation charges have to be introduced and are more or less arbitrarily for the defect calculations.

There are some significant progresses on the quantum mechanic calculations for the electronic structures of solids [1–3]. Among these methods, the simple and efficient tight binding (TB) method has received significant attention and has many applications now. The TB method was used to calculate some complex structures of solids [1,2]. Together with formal KKR method (TB – LMTO) [2,3], the tight binding method was also used in *ab initio* calculations.

In this work, we propose a simple and readily comprehensible method for calculating the electronic structures of solid materials with ionic–covalent type of bonding without using any empirical or adjustable parameter. Major material properties, such as the transferred charge density,

* Corresponding author. Fax: +852 27887791.

E-mail address: heiwong@iee.org (H. Wong).

the position and singular points of allowed energy bands, the width of bandgap, and the threshold energy for photoemission, will also be given. As an example, the method will be used for predicting the electronic structures of amorphous silicon nitride (a-Si₃N₄). Silicon nitride has been the key dielectric used in silicon devices [4–6]. It is also used as the charge storage medium in flash memory cells [7]. To model the structure of a-Si₃N₄, we use the Bethe lattice model with infinitely-extended branches to avoid the requirement for assigning artificial charge localizations. Due to the absence of bond rings, this model substantially simplifies the calculations. It is also found to be quite efficient in predicting the electronic structures of amorphous materials [8,9].

2. Calculation procedures

The tight-binding Hamiltonian used in this calculation is given by

$$\begin{aligned} \hat{H} &= \sum_{ix} \left\{ E_{ix} \hat{c}_{ix}^+ \hat{c}_{ix} + \sum_{j\beta} [V_{ix,j\beta} \hat{c}_{ix}^+ \hat{c}_{j\beta} + \epsilon.c.] \right\} \\ &= \sum_{ix,j\beta} H_{ix,j\beta} \hat{c}_{ix}^+ \hat{c}_{j\beta} + \epsilon.c. \end{aligned} \quad (1)$$

The diagonal and off-diagonal elements of the matrix $H_{ix,j\beta}$ are the major parameters to be determined from the atomic properties of the lattice atoms, changes of the electron localization for forming insulating materials. The changes affect the kinetic and potential energies between the bonding atoms. These energies can be determined using the general quantum-mechanical principles. A heuristic process for determining the diagonal and off-diagonal elements is developed as follow.

2.1. Diagonal matrix elements

The diagonal element $H_{ix,ix} = E_{ix}$ for the i -th lattice site with the wavefunction of the α -th type can be written as

$$H_{ix,ix} = W_{ix} + U_{ix} - T_{ix}, \quad (2)$$

where W_{ix} is the diagonal element of the Hamiltonian for an isolated atom (one-electron atomic level); T_{ix} is the change in the intra-atomic kinetic energy and U_{ix} is the additional Coulomb repulsion energy due to the overlapping of the electron shells of atoms in the material. U_{ix} and T_{ix} can be expressed respectively as

$$U_{ix} = U_{ix}^0 \cdot \left(\frac{a_{0i}}{a_i} \right), \quad T_{ix} = T_{ix}^0 \cdot \left(\frac{a_{0i}}{a_i} \right)^2, \quad (3)$$

where U_{ix}^0 and $T_{ix}^0 = \hbar^2/2m(a_i^0)^2$ are coulomb repulsion energy and the change of intra-atomic kinetic energy for isolated atoms, respectively; a_i^0 is the initial radius of the i th atom, and a_i is the radius of this atom in the solid. The ionic radii of the elements forming the solid material are determined from *ab initio* molecular calculations and from the integer-valued atomic charges. We use quadratic interpolation of the atomic radius based on the charged state of the atom, i.e.,

$$a_i = a_{0i} + a_{1i} \cdot \delta N_i + a_{2i} (\delta N)^2, \quad (4)$$

where δN_i is the change in number of electrons on the atom of the solid; and a_{1i} and a_{2i} were obtained by extrapolating the ionic radii of atoms based on the fraction of charge density. The initial atomic radii a_{0i} were borrowed from the reference data of HyperChem Released 5.02, and the ionic radii $a_i^{\pm q}$ (q are integer numbers) from Ref. [10].

The values of the atomic parameters W_{ix} ($\alpha = s, p$) in (2) were taken from the averaged values of the data calculated from the Hartree–Fock and X_α methods which were reported by Fisher and Hermann, and Skillman, respectively [3] (see Table 1). The Coulomb parameters U^0 (the average intra-atomic Coulomb repulsion of electrons) were adopted from the values reported by Climenti and Roetti [9].

2.2. Off-diagonal matrix elements

The off-diagonal elements can be calculated using the Harrison formula [3] by comparing the free-electron energy bands in the empty lattice with the tight binding energy bands, i.e.,

$$V_{l'l'm} \equiv (ll'm) = \eta_{l'l'm} \cdot \left(\frac{\hbar^2}{m_e} \right) \cdot \left(\frac{1}{d^2} \right), \quad (5)$$

where d is the separation between the nuclei, and $\eta_{l'l'm}$ are the structural parameters defined by the type of the lattice. The subscripts l, l' and m ($=m'$) represent the angular parts of the electron wavefunctions: $l, l' = 0(s), 1(p), 2(d)$, etc; and $m = m' = 0(\sigma), 1(\pi), 2(\delta)$, etc.

Using this expression, we obtain a universal model for the electronic structure of a tetrahedral crystal. In this model, the atomic ‘filling’ of the lattice is defined by the diagonal elements (analogs of atomic levels) only. However, instead of using (5), we use the following formula to calculate the off-diagonal matrix elements,

$$V_{ix,j\beta} = \pm \sqrt{T_{ix} T_{j\beta} n_{ix} n_{j\beta}}, \quad (6)$$

Table 1
Starting values of parameters used for constructing the diagonal matrix elements in the Hamiltonian of Si₃N₄

Atom	Parameters									
	$-W_{is}$	$-W_{ip}$	U^0	a_i^{+5}	a_i^{+4}	a_i^{-3}	a_i^{-4}	a_{0i}	a_{1i}	a_{2i}
Si	14.17	7.05	7.64	–	0.39	–	1.98	1.10	0.199	0.005
N	24.63	12.66	13.15	0.15	–	1.48	–	0.65	–0.255	0.022

where T_{ix} is the change in the intra-atomic kinetic energy, and the occupation numbers are given by

$$N_{ix} = \langle \hat{n}_{ix} \rangle = \langle \hat{c}_{ix}^+ \hat{c}_{ix} \rangle = - \int_{-\infty}^{E_F} \frac{1}{\pi} \text{Im} G_{ix,ix}(E + i0) dE, \quad (7)$$

where $G_{ix,ix}(E + i0)$ is the diagonal matrix element of the one-electron Green function which is the solution of the following system:

$$\sum_{l,\gamma} ((E + i0)\delta_{i,l}\delta_{\alpha,\gamma} - H_{ix,l\gamma}) G_{l\gamma,j\beta}(E + i0) = \delta_{i,j}\delta_{\alpha,\beta}. \quad (8)$$

Note that the off-diagonal matrix elements become dependent on the atomic levels of the initial atoms and on the local coordination of these atoms in the lattice via the occupation numbers. These elements need to be determined in a self-consistent manner. Formula (6) can easily be transformed into (5) using the relationship given below:

$$\eta_{ll'\sigma} = \frac{d^2}{2a_i a_j} (n_{il} n_{j'l'})^{1/2}. \quad (9)$$

The coefficients $\eta_{ll'\sigma}$ playing the role as $\eta_{ll'm}$ in (5). In fact (9) is just used to show the relation with previous reported calculations, it does not need in the present calculations. Table 2 lists the $\eta_{ll'm}$ coefficients calculated with other methods. First row lists the structural factors for the tetrahedral Si lattice given by Harrison using the empty-lattice band structure [3]. Second row depicts the data obtained from semi-empirical calculations on zinc-blende (A3B5) structure materials [9,11]. The subscripts a and c denote the anion and cation, respectively. Data for Si, InAs, and Si₃N₄, calculated in this work using (6) are listed in the third, fourth, and fifth rows of Table 2, respectively. Data in Table 2 indicate that the theoretical data calculated with (6) agree well with those calculations based on adjustable parameters over a wide range of tetrahedral materials. The tight-binding Hamiltonian method, does not need any adjustable parameter, is simple and accurate method for predicting the electronic properties of materials.

2.3. Extended basis

Although the semi-empirical tight binding method is able to describe the valence bands adequately, it fails to give an adequate description of the conduction bands. For nearest-neighbor approximation, it is impossible to

Table 2
Comparison of the factors in $\eta_{ll'm}$ calculated with (9) for various materials and the universal A3B5 tetrahedral structure

$\eta_{ss\sigma}$	$\eta_{sa_p c \sigma}$	$\eta_{sc_p a \sigma}$	$\eta_{pp\sigma}$	$\eta_{pp\pi}$	Material
-1.39	1.88	1.88	3.24	-0.81	Si
-1.38	1.68	1.92	2.20	-0.55	A3B5
-1.42	1.92	1.92	2.58	-0.65	Si
-1.44	1.60	2.01	2.26	-0.63	InAs
-1.27	1.55	1.64	2.01	-0.50	Si ₃ N ₄

predict the band structures of materials with indirect forbidden energy gap [11]. More complicated approximation with larger numbers of empirical parameters may be made, but only little improvement in the conduction band calculation was obtained [2]. Similar difficulties were also found in the non-empirical methods. With this connection, an extended basis consisting both valence orbital and partially-occupied orbital was used. For example, when calculating the Si band structure, d orbits are also taken into account [2,11–13] in addition to sp^3s^* basis which was also used in the semi-empirical calculations [11]. In the semi-empirical approach, the standard sp^3 basis is extended to comprise the excited atomic state s^* with both the diagonal (E_{s^*}) and the off-diagonal (V_{s^*p}) matrix elements which are treated as adjustable parameters. The E_{s^*} and V_{s^*p} parameters are used to fit the structure and the position of the conduction-band edge only as the valence-band structure is less sensitive to these parameters. By performing Leudin transformation the effect of s^* state becomes explicit and the basis extension turns out to be an additive item to the initial Hamiltonian. In matrix form, the additive item can be considered as the atomic interaction with a resonance energy E_{s^*l} extending beyond the nearest neighbors

$$H_{ai,\alpha j}^* = V_{ai,s^*l} \cdot (E - E_{s^*l})^{-1} \cdot V_{sl,\alpha j}, \quad (10)$$

where the subscript l refers to a certain atom site in the lattice with the nearest neighbor lattice site i and the second neighbors site j .

Using the smallest additive energy for valence-band, s^* , and considering the anti-bonding state A^* be the additive to the valence band of type α for the matrix element in (10), we obtain

$$H_{ai,\alpha j}^* = V_{ai,A^*l} \cdot (E - E_{A^*l})^{-1} \cdot V_{A^*l,\alpha j}, \quad (11)$$

where E_{A^*} is the resonance energy for the anti-bonding state in the initial sp^3 basis. Putting (11) into (10) will yield the same results for the second-neighbor interaction as calculated using equations Eqs. (4)–(8). Fig. 1 illustrates the idea of the above treatment.

2.4. Unshared pair

In ionic-covalent materials such as Si₃N₄, the unshared pair $\pi\pi$ orbit plays a special role in determining the width

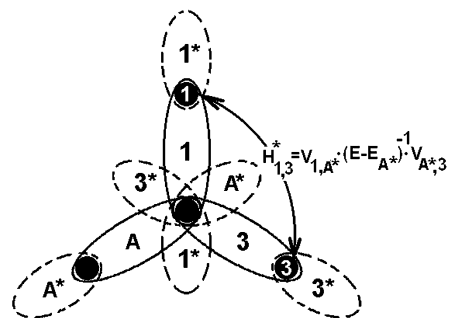


Fig. 1. Sketch illustrating the role of matrix elements in formula (7).

of the bandgap and the position of the valence-band maximum. In conventional tight binding calculations, the diagonal matrix element for the anti-bonding $p\pi$ state was considered as the same as the p state for forming covalent bonds [14,15]. The validity of this treatment is problematic. Electron in anti-bonding state experience a different potential from that of the sp^2 – sp^3 nitrogen–silicon bond. By assuming the diagonal matrix elements due to the $p\pi$ anti-bonding and p bonding states are equal, the energy width $\Delta E_{p\pi}$ of the band formed by unshared pair turns out to be quite narrow when compared to the intra-atomic Coulomb repulsion U_{pN} among electrons. This issue can be overcome by taking the interaction $V_{p\pi N\pi, p\pi N'}$ among the unshared pairs into account [16]. This treatment will result in the $p\pi$ band widening and forbidden band narrowing and the results are closer to the experimental ones. Apart from the adjustable parameters $V_{p\pi N\pi, p\pi N'}$ the self-energy of the unshared pair was also adjusted to have a better correlation between the calculated and experimental results [17].

Using the procedure described in Section 2.3 with silicon–nitrogen bonding, we obtain a parametric relation with the diagonal element $E_{p\pi}$ for $V_{A^*Si, p\pi N}$ and $V_{p\pi N, A^*Si}$,

$$H_{p\pi N, p'\pi N'}^* = V_{p\pi N, A^*Si} \cdot (E_{p\pi} - E_{A^*Si})^{-1} \cdot V_{A^*Si, p'\pi N'} \quad (12)$$

The diagonal element $E_{p\pi}$ itself can be found from Eqs. (2) and (3). The radius of the $p\pi$ state is considered to be equal to the distance between nitrogen atoms. We assume that like in the $N(SiH_3)_3$ molecule, the spreading of the unshared pair formed by p electrons in the $p\pi$ state results in the planar configuration of the nitrogen bonds in silicon nitride.

3. Results

Fig. 2 compares the calculated local density of states with the experimental X-ray emission and absorption spectra for $a\text{-Si}_3\text{N}_4$ reported earlier [18]. The spectra in the figure are normalized with their peak values. The valence-band edge of experimental data lies at -6.5 eV and the energy scale of calculated data was referred to the zero electron energy in the vacuum. To have a better fitting with the shapes of the experimental spectra, the calculated spectra were broadened by adding 0.5 eV to Si 3p, 0.9 eV to Si 3s and N 2p states.

The X-ray emission and absorption spectra of amorphous silicon nitride are depicted in solid lines and the calculated spectra are shown in either dashed or dotted lines in Fig. 2. As shown in Fig. 2, the Si $L_{2,3}$ emission spectrum is due to the transitions from the valence-band electron states with symmetry A_1 . In addition to the s states localized on the Si atom itself (see the dashed curve), the valence band also contributes by a symmetric combination of four $p\pi$ and sp^2 orbital from neighboring nitrogen atoms. The results are depicted in the second plot of Fig. 2. The third plot of Fig. 2 compares the experimental Si K spectrum

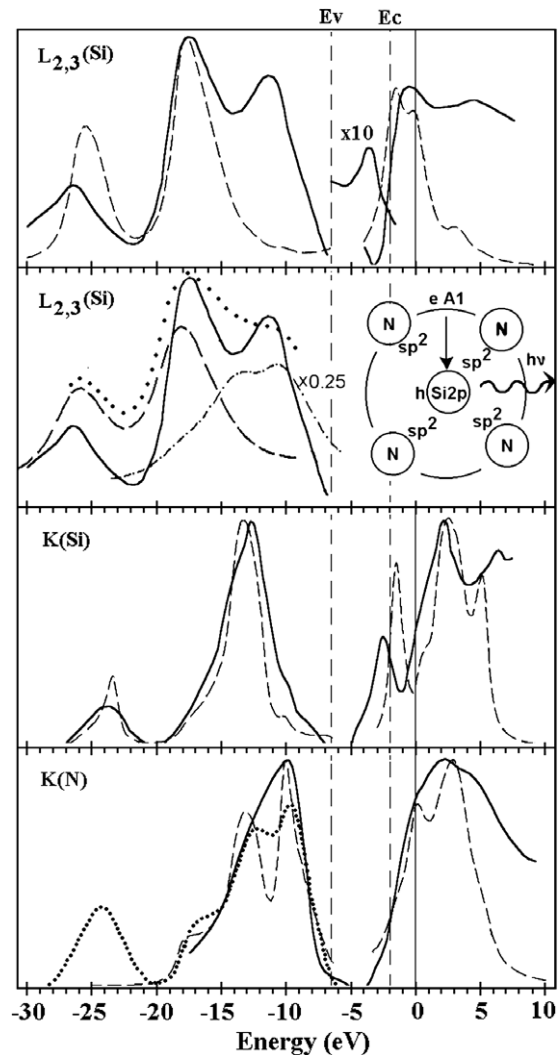


Fig. 2. Comparison of the PDOS calculated with Bethe lattice model with the experimental X-ray emission and absorption spectra of $a\text{-Si}_3\text{N}_4$. Experimental X-ray emission spectra are shown as solid lines. Additional experimental valence band photoelectron spectrum ($h\nu = 87.1$ eV) from Ref. [17] is depicted as dotted line in the lower plot. Other curves are the calculated densities of states.

with the calculated density of p states localized on the Si atom (T_2 symmetry). The fourth plot depicted in Fig. 2 shows the experimental N K spectrum and the calculated density of the p states of the nitrogen atom including the unshared pair. Photoelectron spectrum due to the $a\text{-Si}_3\text{N}_4$ valence band [17] measured using synchrotron radiation with energy of 87.1 eV is also shown. The first peak from the right is believed due to the unshared pair of nitrogen atom.

Fig. 3 shows the normalized total density of states and partial densities of states. The first plot shows the total density of states (solid line) and the weighted sum of the partial densities of states of Si atoms (dashed line) and N atoms (dash-dot line). The second plot shows the partial s (dashed line) and p states (solid line) due to the Si atom. The third plot of Fig. 3 depicts the partial densities of the states due to the nitrogen atom. The s states are plotted in dashed

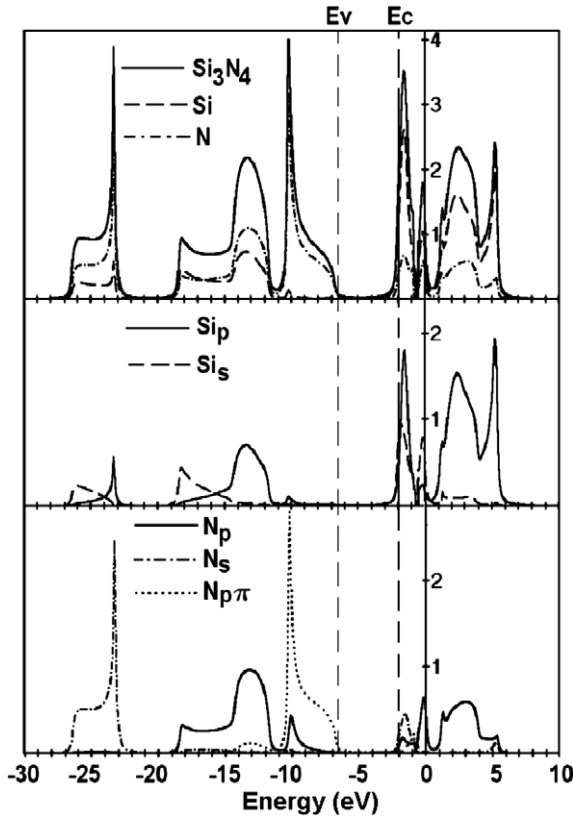


Fig. 3. Normalized PDOS of a-Si₃N₄ calculated using Bethe lattice model. Zero energy is referred to the electron energy in vacuum.

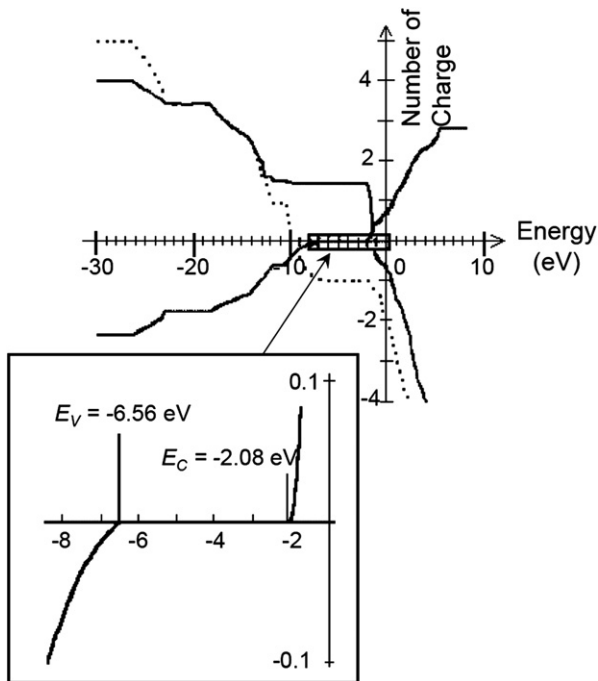


Fig. 4. Charge variations on Si (dash line) and N (dotted line) atoms due to the number of occupation states (in number of electron charge). Solid line represents the charge balance curve as obtained from the weighted summation of charge on Si and N atoms. Inset shows the magnified view of the forbidden band region.

Table 3

Comparison of various the values a-Si₃N₄ parameters calculated in this work and with the experimental values from various sources

Parameters	Calculated	Experimental
Width of the main bandgap (eV)	4.5	4.5 [4]
Ionic gap in the valence band (eV)	4.8	
Charge transfer along the Si–N bond (e)	0.34	0.35 [5]
Position of E_V (eV)	–6.56	–6.5 [4]
Position of E_C (eV)	–2.08	–2.0 [4]
Width of upper valence subband (eV)	11.8	18 [18]
Width of lower valence subband (eV)	3.3	10 [18]

line. The p states for forming the sp^2 – sp^3 bond are shown in solid line and the states of unshared pair are plotted in dotted line.

Fig. 4 illustrates the effect of the charges on the Si and N atoms as a function of the upper limit (E_F) of the integral in (7). The flat portions of the curve correspond to the forbidden bands. The same figure shows the charge balance curve calculated with allowance for stoichiometry $q_b = -(q_{Si}/4 + q_N/3)$. The flat portion of the curve with zero magnitude, with a magnified view shown in the inset, refers to the main bandgap, the edges being the upper edge of the valence band and the lower edge of the conduction band. The numerical results on the band structure of silicon nitride are listed in Table 3.

4. Discussion

It is noted that for calculation of the spectra shown in Fig. 2, weighted summation of the densities of states was used because of the difference between the related matrix elements for the dipole moment operator. Without such weighting, it is hard to obtain a good agreement with the experimental data. Unfortunately, the dipole matrix elements are energy parameter dependent [19] and the relationships are not readily available. In this work, a crude approximation was made by using a single reduction factor for all the components and a much larger (1.8 eV) broadening parameter was used for fitting the calculated data. Taking the measurement accuracies of the experimental data into account, the present theoretical results are still in good agreement with the experimental ones. The major sources of calculation errors are the approximation made for the Hamiltonian, the use of the Bethe lattice, and the accuracies of initial values of the atomic parameters W , U , and a .

In Fig. 3, the singular points of the Si₃N₄ band structure are obvious. The charges q_i on atoms ($i = \text{Si or N}$) were calculated with the formula

$$q_i = Z_i - \sum_{\alpha} n_{i\alpha}(E_F), \quad (13)$$

where Z_i is the number of valence electrons, and expression (7) was used to calculate the second term in (13).

A good agreement between the predicted and experimental values for the band structure of silicon nitride was obtained. Since all energies are calculated from the

single-electron atomic levels and the origin of the energy scale was placed at the energy of electron in vacuum, the calculated results should be accurate enough even considering the surface and many-electron effects. The obtained energy position of the valence-band edge also coincides with the photoemission threshold and the macroscopic photoelectric workfunction.

5. Conclusions

A new tight-binding Hamiltonian calculation was proposed for determining the electronic structures of ionic-covalent materials. The proposed method does not involve any empirical adjustment procedure for determining the band edges and bandgap. The atomic parameters of the solid were determined based on the general quantum principles. Electronic structures of Si_3N_4 were calculated using this method. A good agreement between the calculated and experimental values in terms of fundamental properties such as the absolute position of the valence-band edge, the conduction-band edge, and the energy bandgap were obtained. Charges transfer between the silicon and nitrogen atoms is also precisely calculated in this work.

Acknowledgements

This work was supported by Project No. 97 of Siberian Branch of Russian Academy of Sciences and particularly by Project RFBR No. 06-02-16621.

References

- [1] P.E.A. Turchi, A. Gonis, and L. Colombo (Eds), in: MRS Proc., 491: Tight-Binding Approach to Computational Materials Science, 1998.
- [2] O.K. Andersen et al., in: P.E.A. Turchi, A. Gonis, L. Colombo (Eds.), MRS Proc., 491: Tight-Binding Approach to Computational Materials Science, 3, 1998.
- [3] W.A. Harrison, *Electronic Structure and the Properties of Solids*, W.H. Freeman & Co, San Francisco, 1980.
- [4] V.A. Gritsenko, in: *Silicon Nitride in Electronics*, Elsevier, New-York, 1988, p. 138.
- [5] V.A. Gritsenko, *Structure and Electronic Structure of Amorphous Dielectrics in Silicon MIS Structures*, Nauka, Novosibirsk, 1993.
- [6] H. Wong, H. Iwai, *Microelectron. Eng.* 83 (2006) 1867.
- [7] V.A. Gritsenko, K.A. Nasyrov, Yu.N. Novikov, A.L. Aseev, S.Y. Yoon, J.-W. Lee, E.-H. Lee, C.W. Kim, *Solid-State Electron.* 47 (2003) 1651.
- [8] R.B. Laughlin, J.D. Joannopoulos, D.J. Chadi, *Phys. Rev. B* 20 (1979) 5228.
- [9] J.A. Majewski, P. Vogl, *Phys. Rev. B* 35 (1987) 9666.
- [10] M.I. Shaskol'skaya, *Crystallography*, Vysshaya Skola, Moscow, 1976.
- [11] P. Vogl, H.P. Halmanson, J.D. Dow, *Chem. Solids* 44 (1983) 365.
- [12] V.A. Gritsenko, Yu.N. Novikov, A.V. Shaposhnikov, Yu.N. Morozov, *Fiz. Tekhn. Poluprov* 35 (2001) 1041.
- [13] S.-Y. Ren, W.Y. Ching, *Phys. Rev. B* 23 (1981) 5454.
- [14] E.C. Ferreira, C.E.T. Goncalves da Silva, *Phys. Rev. B* 32 (1985) 8332.
- [15] J. Robertson, *Philos. Mag.* B 63 (1991) 47.
- [16] L. Martín-Moreno, E. Martínez, J.A. Vergés, F. Yndurain, *Phys. Rev. B* 35 (1987) 9683.
- [17] R. Karcher, L. Ley, R.L. Johnson, *Phys. Rev. B* 30 (1984) 1896.
- [18] V.A. Gritsenko, Yu.N. Morokov, Yu.N. Novikov, *Appl. Surf. Sci.* 113&114 (1997) 417.
- [19] I.A. Brytov, V.A. Gritsenko, Yu.N. Romashchenko, *JETP* 62 (1985) 321.